DESIGN OF A HIGH PERFORMANCE HAPTIC INTERFACE TO VIRTUAL ENVIRONMENTS

P.A. Millman, Michael Stanley, J. Edward Colgate
Department of Mechanical Engineering
Northwestern University, Evanston, IL 60208

Abstract *– The design of a four degree-of-freedom, force-reflecting manipulandum for manual interaction with virtual environments is presented. The device emulates a handtool which the operator can use to explore and manipulate virtual objects. The performance of the device, its ability to generate a broad range of impedances, is determined by a variety of factors including the inherent dynamics of the manipulator, the accuracy and resolution of sensors, and the speed of the digital controller.*

1. Introduction

A force-reflecting manual interface, or manipulandum, is essentially a joystick that enables a human operator to interact with dynamic systems, virtual or real, through the haptic sense. In a common implementation, motions of the manipulandum endpoint (handle) provide motion commands to a "slave" manipulator which might be a robot, a micromanipulator, or a computer simulated tool in a virtual environment. Interaction forces computed by the simulation, or measured at the endpoint of the real slave manipulator, are fed back as force commands to the manipulandum. In this type of system the manipulandum can be thought of as a force display.

Systems of this sort have been used to implement a variety of environments. For example Minsky et.al. use a two degree-of-freedom (DOF) joystick to create the feel of sandpaper, viscous soups, springs and yo-yos [7]. Cadoz et al. describe a one degree-of-freedom "piano key" for stroking, plucking, and striking virtual musical strings [3]. A handheld device built by Burdea uses pneumatic cylinders attached between the palm and fingers to simulate the feel of squeezing rubber balls and deforming aluminum cans [2]. Adelstein implements environments such as springs, dampers, and walls with a two DOF joystick to study human arm tremor [1], and Jones and Hunter use a one DOF manipulandum to study human perception of stiffness and damping [6]. The challenges of building a high performance haptic interface, which will be discussed in Section 2, have limited most of these devices to one or two degrees-of-freedom.

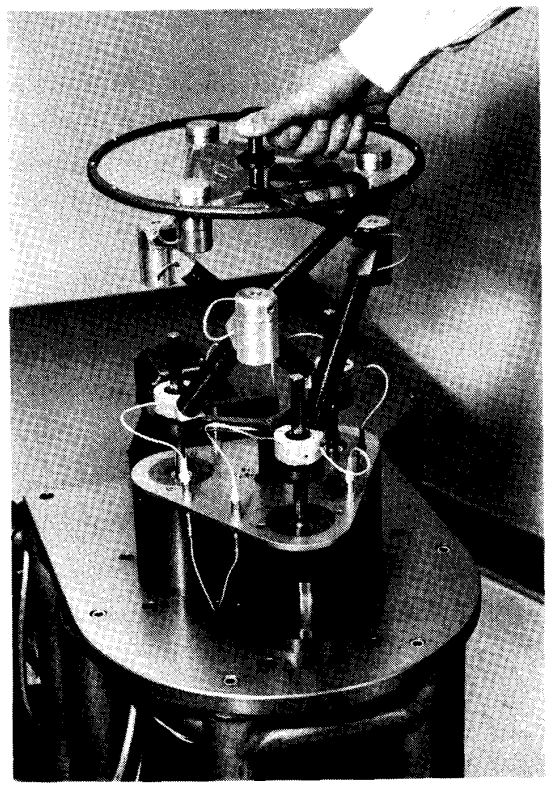

Figure 1. Manipulandum

0-7803-1363-1/93 $3.00 © 1993 IEEE

2. Motivation

This paper describes a manipulandum that was designed as part of a system to emulate hand tools used to perform various mechanical tasks. Users grasping the handle of the manipulandum interact with a virtual environment using a virtual tool, and feel the forces of that interaction at the handle of the manipulandum. Possible simulations include tightening a nut onto a bolt with a wrench and assembling a virtual jigsaw puzzle. These simulations are representative of a class of environments being investigated that comprise rigid bodies interacting with one another [8]. Other system components include digital control processors, environment simulation processors, a host computer, and a graphical display.

3. Mechanical Design

To simulate a wide variety of mechanical environments, the manipulandum must be able to exhibit widely varying mechanical impedances across a broad frequency range. If endpoint forces are open-loop controlled, the lower limit on the device's impedance is simply its inherent backdriveability. Closed-loop endpoint force control can partially mask the inertia and friction of the machine, but the inherent dynamics of the mechanism will still limit backdriveability because of stability issues [5]. For these reasons, low inertia and low friction are important design criteria.

To generate high impedances (such as stiff springs, large inertias and hard walls) the device needs to be mechanically stiff and the actuators must have large, high-bandwidth force generating capabilities. Also, low structural stiffness and high inertia result in low natural frequencies for the manipulator, which can cause closed-loop instability when force sensors and actuators are noncollocated. Backlash in the transmission can also be a cause of instability. Other considerations in the mechanical design include range of motion and degrees-of-freedom suitable to the performed tasks and the simulated environments. Greater freedom of motion is clearly advantageous for implementing interesting virtual environments.

In addition to these mechanical considerations, sensor resolution and controller update rate both affect stability of high impedance simulations. Sensor resolution will be discussed in more detail in Section 4, and controller update rates in Section 5.

3.1 Kinematics

The mechanism allows translation in three directions, and rotation in the horizontal plane. Although full freedom of motion would be ideal, many interesting tasks (such as putting a nut on a bolt or assembling a jigsaw puzzle) do not require tilting. A closed-chain mechanism provides the manipulandum's three planar degrees-of-freedom (Fig. 2) and a prismatic joint at the base of the planar mechanism allows vertical translation. The three revolute joints at the base of the planar mechanism are actuated through low friction, zero-backlash ball splines which transmit torque from three DC motors to the three lowest links but do not restrict vertical translation of the planar mechanism (Fig. 1). The other six revolute joints of the planar mechanism are not actuated.

A fourth motor generates vertical forces on the manipulator via a pulley and steel belt drive train. The steel tapes drive a "Y"-shaped *triad* that constrains the spline nuts to move vertically as a unit, but allows them to rotate independently.

The closed-chain kinematics result in some very desirable features. Most importantly, all four motors are base-mounted, resulting in low link inertia without actuators that are remotized via complicated tendon or belt transmissions. The parallel structure is also more rigid than serial designs. The device is direct drive in order to maximize backdriveability and stiffness and to eliminate backlash. Gearing down actuators limits backdriveability because of friction and amplification of motor inertia felt by the operator through the transmission.

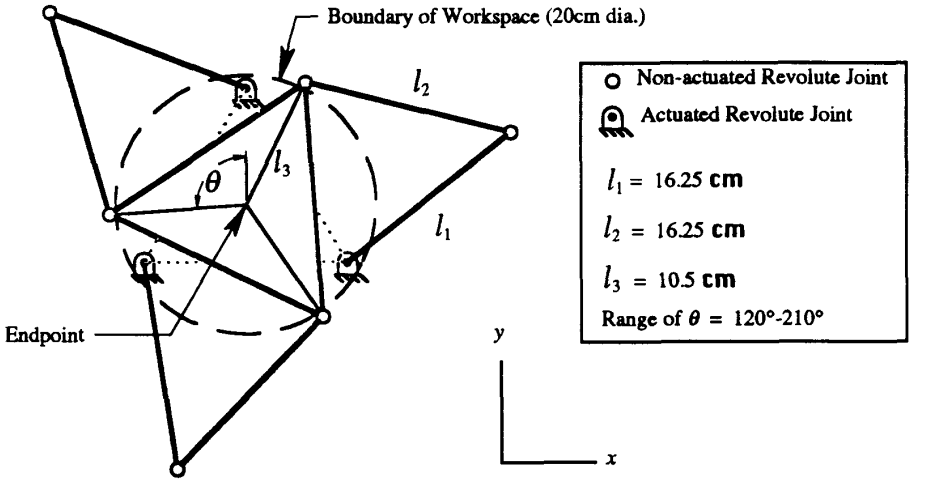

Figure 2. Kinematic diagram of planar, parallel-link mechanism.

The planar mechanism is designed for the following ranges of motion: horizontal translation within a 20 cm (8 in.) diameter circle, vertical translation of 8.5 cm (3.5 in.), and rotation of ±45°. Static endpoint loads of 45 N (10 lbs) and 135 N-cm (12 in-lbs) can be generated throughout the workspace.

The lengths of the links were selected to minimize both the required actuator torques and the size of the links themselves, while ensuring that the above design constraints on endpoint motion and force were met. The main reasons for selecting a design that required minimum actuator torques were to save space and cost. Short links were desirable to minimize compliance and inertia. Also, endpoint position resolution was improved with shorter links because joint motions were more sensitive to motions at the endpoint. The kinematic parameters were selected after numerically evaluating actuator torques at points throughout the workspace for over 500 different kinematic designs. The technique also ensured that the workspace was free of singularities. Potential problems of interference between links were examined by constructing a full scale wooden model of the mechanism.

3.2 Actuators

Brushless DC motors (Robins and Meyers/Electro-Craft) were selected for their small size, low friction, and low inertia compared to brushed motors of equal torque output. They also exhibit no reluctance cogging or torque ripple that would add noise to the force output of the manipulandum.

3.3 Links

The links of the manipulator were designed to optimize their stiffness-to-mass ratio. An optimal design maximizes the natural frequencies of the structure, to help prevent excitation of those modes, especially under closed-loop endpoint force control. Filament-wound graphite composite tubes with an axial modulus of elasticity of 120 GPA (1.7 times aluminum) and density of 1600 kg/m^3 (0.6 times aluminum) were used for their superior mechanical properties compared to metals. The links were bonded to the aluminum joints with epoxy adhesive.

Lumped-parameter models of the manipulandum's structural dynamics were developed to predict the natural frequencies of the mechanism, given estimates of link stiffnesses and joint masses. Two parameters, tube diameter and wall thickness, were varied to maximize the lowest natural frequency of the models. The final design had a lowest natural frequency of ~100 Hz.

3.4 Vertical Drive

The components of the vertical drivetrain, including the triad and steel drive tape, were designed using similar lumped-parameter models to estimate natural frequencies. Stainless steel tapes provide a stiff transmission with negligible friction, and zero backlash. "Constant force" springs effectively counterbalance the weight of the mechanism and add very little inertia and friction.

In summary, the kinematic design of the manipulandum involved a number of tradeoffs involving both static and *dynamic* properties of the device. The mechanical components of the device were also carefully selected or designed for high mechanical bandwidth (i.e. high natural frequencies) and precise control of endpoint forces.

4. Sensors

Optical encoders on the motors and precision potentiometers at the non-actuated joints sense angular positions of the joints. The potentiometers are extremely compact, lightweight, and low torque. Although joint angles from the optical encoders are sufficient to compute endpoint position and orientation as well as the Jacobian, having all nine joint angles greatly simplifies (and speeds) the computations. The redundant information also provides the opportunity to check for faulty sensor readings in real time.

Sensor resolution, particularly velocity resolution, is an issue of great importance regarding stability. We take as anecdotal evidence experiments performed in our lab with a one degree-of-freedom device consisting of a lever arm driven by a DC motor. The damped walls we implemented were very unstable and the forces generated were very erratic. This was because implementing effective virtual damping relies on a low noise velocity signal which we were unable to get by numerically differentiating shaft position as measured by an 8000 counts/rev optical encoder. The reason for this was clear after calculating the minimum resolution of the velocity measurement, which is the position resolution divided by the time step of the controller, $V_{res} = X_{res}/T$. Using encoders with 8000 counts/rev and running the control algorithm at 1 KHz meant that the velocity could only change in multiples of 7.9×10^{-4} rad/0.001 sec = 0.79 rad/sec (45°/sec)! Increasing the update rate only made velocity resolution worse, making the spikes in the damping force taller although narrower and perhaps more easily filtered by the inertia of the mechanism. Differentiating position twice to get acceleration would obviously have been unwise. For a more complete discussion of sources of instability when implementing stiff virtual walls see [4]

The motors of the manipulandum have been fitted with high resolution optical encoders with 900,000 counts/rev (Teledyne Gurley Series 835 encoder and HR2 interpolator) to improve velocity resolution. Motor position resolution is now 7.0×10^{-6} radians and velocity resolution is 7.0×10^{-3} rad/sec. This resolution is comparable to using a tachometer with a 15 bit A/D converter and a maximum motor velocity of 20 rad/sec. Position resolution of the passive joints is 11 bits of A/D over a range of 120°, or 1.0×10^{-3} radians. Position resolution is more important at the motors than at the other joints because we calculate endpoint velocity by multiplying the motor velocities by the inverse Jacobian, instead of differentiating endpoint position.

Equation (1) is the expression for endpoint velocity, $\dot{x}$, in terms of motor velocities, $\dot{\phi}$, and the Jacobian, J.

$$\dot{x} = J^{-1}\dot{\phi}, \tag{1a}$$

$$\begin{bmatrix} V_x \\ V_y \\ V_\theta \end{bmatrix} = \begin{bmatrix} c_{11} & c_{12} & c_{13} \\ c_{21} & c_{22} & c_{23} \\ c_{31} & c_{32} & c_{33} \end{bmatrix} \begin{bmatrix} \dot{\phi}_1 \\ \dot{\phi}_2 \\ \dot{\phi}_3 \end{bmatrix} \tag{1b}$$

Variations in the endpoint velocities are caused by variations in the terms of the Jacobian and variations in motor velocities. The motor velocities change in discrete steps, as discussed, of $7.0\text{x}10^{-3}$ rad/sec. The terms of the Jacobian also change in discrete fashion due to the discretization of the joint angles either by the D/A converters or the optical encoders. The sensitivity of the Jacobian to changes in joint angles is different at different locations in the workspace. We can express a variation in velocity, denoted δV as

$$\delta V = \delta J\dot{\phi} + J\delta\dot{\phi} \; . \tag{2}$$

Multiplying out these terms, the variation in V_x, denoted δV_x, is

$$\delta V_x = \delta c_{11}\dot{\phi}_1 + \delta c_{12}\dot{\phi}_2 + \delta c_{13}\dot{\phi}_3 + c_{11}\,\delta\dot{\phi}_1 + c_{12}\,\delta\dot{\phi}_2 + c_{11}\dot{\phi}_1 \; . \tag{3}$$

Regrouping terms, the resolution of V_x is

$$\delta Vx = (|c_{11}| + |c_{12}| + |c_{13}|)\delta\dot{\phi} + (\delta c_{11} + \delta c_{12} + \delta c_{13})\dot{\phi} \; , \tag{4}$$

where $\delta\dot{\phi}$ is the motor velocity resolution, and the velocities of all three motors are assumed to be equal. The term $(\delta c_{11} + \delta c_{12} + \delta c_{13})$ will be maximized at a particular combination of incremental changes in the nine joint angles of $1.0\text{x}10^{-3}$ radians. δVy and δV_θ can be expressed similarly.

Endpoint velocity resolution was evaluated numerically at different points in the workspace to determine its relative sensitivity to motor velocity resolution and joint angle resolution. Fig. 3 shows the maximum possible values of the two terms of (2). The first term is constant with motor speed and the second increases linearly with motor speed.

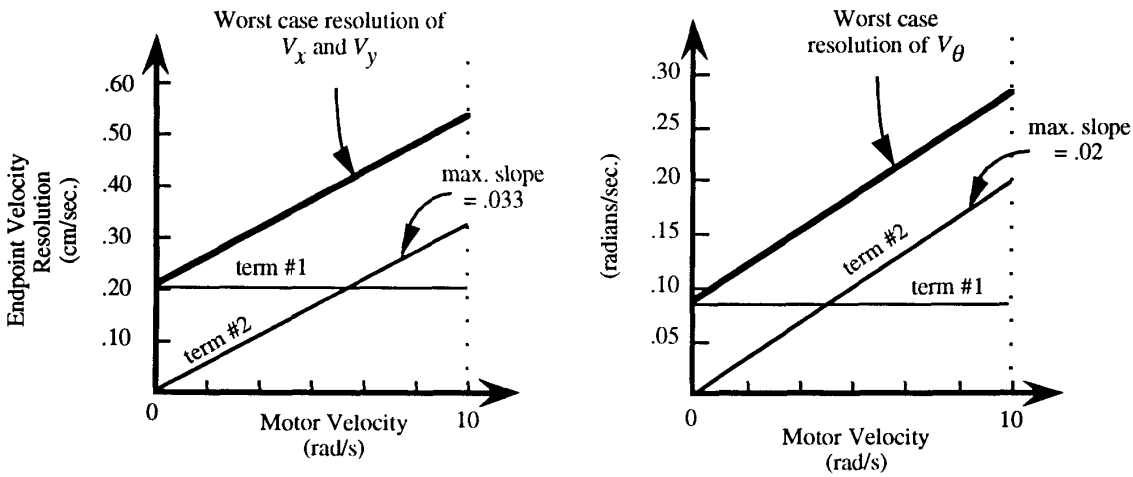

Figure 3. Resolution of endpoint translational (a) and rotational (b) velocities.

Resolution is plotted up to 10 rad/sec which is approximately the maximum motor velocity that a person can generate by moving the endpoint. Improving the position resolution of the potentiometers by a factor of two reduced the slope of the second term by one-half (i.e. the relation was approximately linear). It is worth noting that these maximum values were encountered at the extreme edges of the workspace. Over a majority of the workspace the contribution of each term was about one half the maximums shown. As a comparison between linear and angular velocity resolution, 0.2 cm/sec is the translational velocity resolution at the end of a 28 cm (11 in.) long moment arm attached to the shaft of a high resolution encoder with velocity resolution of 7.0×10^{-3} rad/sec.

5. Control

The backbone of the computer system for the manipulandum is a VMEbus. The VMEbus facilitates communication between I/O devices, real-time processors and an embedded PC used for code development. All of the real-time computations for manipulator control and virtual environment simulations are executed on a network of distributed-memory, parallel processors called transputers. The basic component of the network is the Inmos T805 Transputer [Inmos], which is a 32-bit processor running at 30 MHz clock speed. It provides a sustained instruction rate of 15 MIPS (30 MIPS peak). A 64-bit floating point coprocessor provides a sustained rate of 3.3 MFLOPS (4.3 MFLOPS peak). Each transputer includes four high speed bi-directional serial links for interprocessor communication. The links operate at a rate of 20 Mbits/sec and can achieve a throughput of 2.4 Mbytes/sec.

Four transputers are dedicated to control of the manipulator. This control subsystem performs the kinematic calculations necessary to determine endpoint position and velocity from the joint angles of the manipulator. It also calculates the inverse Jacobian transpose to determine the motor torques required to produce specified endpoint forces and torque. All I/O across the VMEbus to external devices like encoders, potentiometers, and motor controllers is handled by the control subsystem. The control subsystem also monitors the endpoint position to make sure the manipulandum stays within its workspace. Since this function overrides the other outputs, it has been called *reflex control*. More will be said about reflex control in Section 6.

The endpoint position and reflex control algorithms together were timed as executing at 2000 Hz, and the Jacobian calculation alone was timed at 3000 Hz. These did not include reading joint angles from the pots and encoders, but after the I/O is included the update rates should still be greater than 1000 Hz.

6. Safety

A primary concern in the design of the system was the safety of the operator who interacts with this very powerful machine. Another concern was that the machine can damage itself if it moves beyond the specified boundaries of its workspace, where link interference and joint reversals are possible. Three types of measures are in place to prevent accidents during operation: mechanical stops and covers, hard-wired enable/disable circuitry, and software control.

A 12 in. diameter polycarbonate disk covering the top of the manipulator (see Fig. 2) keeps hands away from moving links. Mechanical stops built into the face plate and shaft coupling of the vertical drive motor keep the device in a safe range of vertical translation. The other motors do not have mechanical stops to limit their motion because the stops cannot be configured to provide any significant protection against the manipulandum moving outside its workspace. To meet that need, reflex control implements virtual walls bounding the acceptable workspace.

A number of safety features are implemented at the level of hardwired circuitry that enables or disables the four motors simultaneously. Torque limits and velocity limits can be set at the amplifiers. Accelerometers have been mounted on the driven links, and an electronic circuit has been built that will disable the motors in the event of dangerously high ballistic acceleration, while allowing decelerations of the type that occur when striking a virtual wall. The circuit will detect overthreshold accelerations in a frequency range of 0-100 Hz within 2 ms. Momentary switches on the handle of the manipulandum and in the operator's free hand must also be closed for the motors to be enabled.

Conclusions

A four degree-of-freedom manipulandum was built to facilitate research in virtual environments, teleoperation, psychophysics, and biomechanics. The performance of the device, its ability to simulate a wide range of impedances, is determined by a variety of factors including the inherent dynamics of the mechanism and its actuators, the accuracy and resolution of sensors, and the speed of the control loop. Future work will include use of an endpoint force sensor for masking the inherent friction and inertia of the mechanism and for implementing large impedances.

Acknowledgements

The authors gratefully acknowledge the support of the Engineering Foundation, Grant RI-A-90-4, and the National Science Foundation, Grant MSS-9022513.

References

1. Adelstein, B. A. and M. J. Rosen. *Design and Implementation of a Force Reflecting Manipulandum for Manual Control Research.* ASME Winter Annual Meeting. Anaheim, California (1-12) (1992)
2. Burdea, G., JZhuang, E. Roskos, D. Silver and N. Langrana. *A Portable Dextrous Master with Force Feedback.* Presence **1**(1):18-28 (1992)
3. Cadoz, C., A. Luciani and J. Florens. *Responsive Input Devices and Sound Synthesis by Simulation of Instrumental Mechanisms: The Cordis System.* Computer Music Journal **8**(3):60-73 (1984)
4. Colgate, J. E., P. Grafing and M. Stanley. *Implementation of Stiff Virtual Walls in Force-Reflecting Interfaces.* IEEE Virtual Reality Annual International Symposium. Seattle, Washington (1993)
5. Colgate, J. E. and N. Hogan. *Robust Control of Dynamically Interacting Systems.* International Journal of Control **48**(1):65-88 (1988)
6. Jones, L. A. and I. W. Hunter. *A Perceptual Analysis of Stiffness.* Experimental Brain Research **79**:150-156 (1990)
7. Minsky, M., M. Ouh-young, O. Steele, J. F. P. Brooks and M. Behensky. *Feeling and Seeing: Issues in Force Display.* Association for Computing Machinery :235-243 (1990)
8. Stanley, M. and J. E. Colgate. *Real Time Simulation of Stiff Dynamic Systems via Distributed Memory Parallel Processors.* IEEE Virtual Reality Annual International Symposium. Seattle, Washington (1993)